Zeitschrift für Kristallographie, Bd. 135, S. 18—33 (1972)

# $\gamma$ $Na_2BeF_4$, its crystal structure at 25° and 74°C and its anisotropic thermal expansion

By S. DEGANELLO

Department of Geophysical Sciences, The University of Chicago*

(Received 20 July 1971)

**Auszug**

Die thermische Ausdehnung von $\gamma$ $Na_2FeF_4$ bis 140°C wurde mit einer Guinier-Lenné-Kamera gemessen. In der Datenanalyse — mit einem platinkalibrierten Film ausgeführt — wurden nur die scharfen Linien berücksichtigt, die eindeutig Cu$K\alpha_1$-Emissionslinien waren. Die Verfeinerung der Strukturen bei 25° und 74°C weist auf eine Temperaturabhängigkeit der $U$-Werte hin, die nicht mit den Ausdehnungsdaten übereinstimmt. Werden aber die Änderung der Bindungslängen bei 25° und 74°C und der Mittelwerte der Amplituden berücksichtigt, so läßt sich die Erscheinung qualitativ verstehen. Der höhere Wert der mittleren Schwingungsamplitude entlang $c$ weist diese Achse als Vorzugsrichtung des Streßnachlassens beim Aufheizen aus. Die Ausdehnung entlang $b$ wird von der Starrheit der M(1)-Polyeder, die um Inversionszentren gelegen sind, gehemmt und wirkt somit den kooperativen Erscheinungen der Translationsbewegung entlang dieser Achse entgegen. Wegen der Stabilität der tetraedrischen Konfiguration ist die Ausdehnung entlang $a$, wie theoretisch erwartet, am kleinsten. Die plötzliche Zunahme von $\alpha_1$ bei 120°C wird der Bildung eines starken Abstoßungspotentials zugeschrieben; dieses stammt vom Wechsel von einer $sp^3$-Konfiguration der Tetraeder-Bindungen zu einer Konfiguration mit kleineren Werten der Orbitalhybridisation. Die dichte Packung steht diesem Wechsel im Wege, und bei einer kritischen Temperatur sollte eine Phasenänderung eintreten. Bei 187 $\pm$ 5°C wird die Umwandlung in eine monokline Phase beobachtet.

**Abstract**

The thermal expansion of $\gamma$ $Na_2FeF_4$ was measured up to 140°C using a Guinier-Lenné camera. Refinement of the crystal structure at 25° and 74°C indicates a temperature dependence of the $U$'s not in agreement with the expansion data. However, consideration of the changes in bond lengths at 25° and 74°C and of the values of the root-mean-squared amplitudes allows a qualitative understanding of the phenomenon. The higher value of the root-mean-squared amplitudes along $c$ positively fix the latter as a preferential direction of

* Chicago, Illinois 60637.

stress relief upon heating. Expansion along $b$ is controlled by the rigidity of the M(1) polyhedra located at inversion centers and opposing cooperative phenomena of translational motion along this direction. Due to the stability of the tetrahedral configuration controlling the $a$ repeat, expansion along $a$ is the smallest one, in agreement with theoretical expectations. The abrupt increase in $\alpha_1$ at 120 °C is attributed to the formation of a stronger repulsion potential caused by a change from a $sp^3$ configuration of the tetrahedral bonds to one tending toward lower values of orbital hybridization. This process opposes the close-packed arrangement and at a critical temperature a phase change is expected to take place. This is in agreement with the experimental data since at 187 $\pm$ 5 °C an inversion to a monoclinic phase was positively identified.

## Introduction

$\gamma$ $Na_2BeF_4$ is isotypic with forsterite (HANKE, 1965) and because of the relatively low upper temperature of its stability field (187 $\pm$ 5 °C) it is well suited for high-temperature studies. In order to obtain information on the temperature dependence of the structural parameters, three-dimensional measurements were made at 25 °C and 74 °C. The results were interpreted in terms of changes of the thermal and positional parameters and discussed in relation to the anisotropic thermal expansion of the structure.

## Data determination

### Powder diffractometry

The lattice parameters at room and high temperature were computed from powder data obtained with a Guinier-Lenné camera with an x-ray chamber evacuated by a mechanical pump to reduce air scattering. Only sharp lines unequivocally due to the Cu$K\alpha_1$ emission line were considered in the analysis while lines due to the platinum sample holder were used for calibration since its coefficients of thermal expansion are well known (CAMPBELL, 1962). The temperature in the sample chamber was stabilized for about two hours prior to exposure to x-rays at each temperature up to a maximum temperature of 140 °C. All lines were recorded on the same film and unambiguously indexed with the aid of three-dimensional intensity data. The lattice parameters were refined by the method of the least squares using the computer-program LSQ (BUSING *et al.*, 1962) with the IBM 7094 computer. The final values at 25 °C are: $a$ = 4.8946(8) Å, $b$ = 10.9253(7) Å, $c$ = 6.569(1) Å. Since thermal expansion is very uniform up to 96 °C (the temperature which marks an abrupt increase in $a$), the mean values

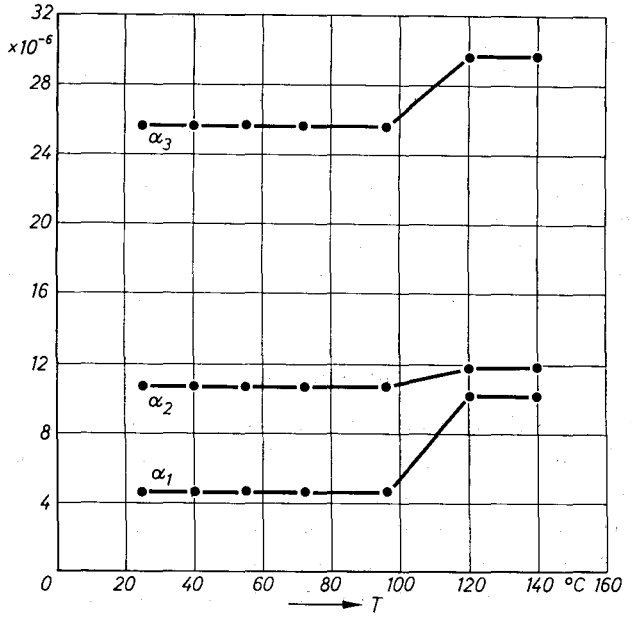


Fig. 1. Temperature dependence of the principal coefficients of thermal expansion

of the expansion coefficients along the three principal crystallographic directions, both for the temperature ranges 25°—96° and 25°—140°C were computed. The final values are:

$$\alpha_{1(25°-96°C)} = 4.7 \times 10^6\,°C^{-1} \qquad \alpha_{1(25°-140°C)} = 7.4 \times 10^6\,°C^{-1}$$
$$\alpha_{2(25°-96°C)} = 10.6 \times 10^6\,°C^{-1} \qquad \alpha_{2(25°-140°C)} = 11.2 \times 10^6\,°C^{-1}$$
$$\alpha_{3(25°-96°C)} = 25.6 \times 10^6\,°C^{-1} \qquad \alpha_{3(25°-140°C)} = 25.6 \times 10^6\,°C^{-1}.$$

The results are summarized in Table 1 and Fig. 1.

Table 1. *Temperature dependence of the lattice parameters at room and high temperature*

| $T$ | $a$ | $b$ | $c$ | Cell volume, $a \cdot b \cdot c$ | Axial ratio |
|---|---|---|---|---|---|
| 25°C | 4.89461 (87) Å | 10.92536 (73) Å | 6.5692 (13) Å | 351.29 (4) Å$^3$ | 0.4480:1:0.6012 |
| 41 | 4.89498 (79) | 10.92723 (66) | 6.5719 (12) | 351.52 (4) | 0.4479:1:0.6014 |
| 57 | 4.89535 (75) | 10.92910 (62) | 6.5746 (11) | 351.75 (3) | 0.4479:1:0.6015 |
| 73 | 4.89572 (74) | 10.93097 (61) | 6.5773 (11) | 351.98 (3) | 0.4478:1:0.6017 |
| 96 | 4.89609 (77) | 10.93284 (64) | 6.5800 (12) | 352.21 (3) | 0.4478:1:0.6018 |
| 120 | 4.89943 (41) | 10.93655 (34) | 6.58739 (65) | 352.97 (2) | 0.4479:1:0.6023 |
| 140 | 4.90387 (08) | 10.94251 (35) | 6.58746 (15) | 353.487 (9) | 0.4481:1:0.6020 |

### Single-crystal diffractometry

$\gamma$ $Na_2BeF_4$ exhibits orthorhombic morphology with forms {001}, {101}, {010} etc. Preliminary precession photographs unambiguously confirmed extinction criteria attributable to the space group *Pbnm*. Three-dimensional intensity measurements were made using a crystal .17 × .38 × .06 mm mounted on the join of a Pt-PtRh 10% thermocouple and aligned along the [010] direction on a PAILRED automated diffractometer. Using monochromated molybdenum radiation from a graphite monochromator, 14 levels of data (1495 intensities) were measured at 25 °C and eleven levels (1246 intensities) were measured at 74 °C. Half-scan ranges of 2° 0′ and 2° 20′, respectively, were used for the low- and high-angle reflections and subsequently increased to 2° 20′ and 2° 50′ for data measurement at high temperature, to accommodate the expected broadening of the Bragg peaks. The heating element was a $N_2$ gas-coil, serpentine heater operating at a gas pressure of about 35 psi. The temperature control is considered better than ± 3 °C. Because of the favorable crystal shape and low value of $\mu$ (0.5 $cm^{-1}$), absorption corrections were not made.

### Structure refinement

The intensities measured at 25 °C were refined by the method of full-matrix, least squares using a locally modified version of ORFLS (Busing *et al.*, 1962) for the 7094 computer. The structural parameters reported by Birle *et al.* (1968) for forsterite were used initially while values for the atomic scattering factors accounting for anomalous scattering of sodium and modified for half ionization were taken from MacGillavry and Rieck (1962). After three preliminary cycles of refinement, the conventional discrepancy index $R$ converged to 0.15. After rejection of few reflections obviously suffering from extinction, $R$ dropped to 0.11. Since weak- and medium-intensity reflections are particularly affected by multiple-reflection effects (Zachariasen, 1965), the data were checked very carefully. In case of suspected contribution from Renninger effects, the corresponding reflection was rejected. A subsequent refinement rapidly converged to $R = 0.08$ which eventually dropped to 0.06 after allowance for isotropic temperature motion. A final anisotropic refinement converged to $R = 0.049$ and a difference Fourier map at this point did not show any anomalous peak or through. The same procedure was used to refine the intensities measured at 74 °C except that the final low-temperature structural

Table 2. *Atomic parameters at 25° and 74°C*

| | 25°C | 74°C | $\Delta$ | $\sigma_{25°C}$ | $\sigma_{74°C}$ | $B_{25°C}$ | $B_{74°C}$ |
|---|---|---|---|---|---|---|---|
| Na(1) | | | | | | | |
| $x$ | 0 | 0 | | — | — | | |
| $y$ | 0 | 0 | | — | — | 1.56 Å$^2$ | 1.65 Å$^2$ |
| $z$ | 0 | 0 | | — | — | | |
| Na(2) | | | | | | | |
| $x$ | 0.9880 | 0.9878 | −0.0002 | 0.0010 | 0.0018 | | |
| $y$ | 0.2801 | 0.2803 | 0.0002 | 0.0005 | 0.0009 | 1.40 | 1.28 |
| $z$ | 0.25 | 0.25 | 0.0 | — | — | | |
| Be | | | | | | | |
| $x$ | 0.4254 | 0.4214 | −0.004 | 0.0031 | 0.0005 | | |
| $y$ | 0.0964 | 0.0951 | −0.0013 | 0.0016 | 0.0032 | 0.91 | 1.42 |
| $z$ | 0.25 | 0.25 | 0.0 | 0.0 | 0.0 | | |
| F(1) | | | | | | | |
| $x$ | 0.7415 | 0.7433 | 0.0018 | 0.0015 | 0.0026 | | |
| $y$ | 0.0934 | 0.0930 | −0.0004 | 0.00077 | 0.0014 | 1.48 | 1.25 |
| $z$ | 0.25 | 0.25 | 0.0 | — | — | | |
| F(2) | | | | | | | |
| $x$ | 0.1960 | 0.1977 | 0.0017 | 0.0015 | 0.0024 | | |
| $y$ | 0.4636 | 0.4660 | 0.0024 | 0.0007 | 0.0013 | 1.36 | 1.57 |
| $z$ | 0.25 | 0.25 | 0.0 | — | — | | |
| F(3) | | | | | | | |
| $x$ | 0.3057 | 0.3065 | 0.0008 | 0.0010 | 0.0017 | | |
| $y$ | 0.1613 | 0.1616 | 0.0003 | 0.00055 | 0.00098 | 1.42 | 1.53 |
| $z$ | 0.0596 | 0.0606 | 0.0001 | 0.00077 | 0.0013 | | |

parameters were used as initial input. After correction for Renninger effects and allowance for isotropic temperature motion the conventional $R$ was 0.07. A weighting scheme suggested by CHESSIN *et al.* (1965) was adopted. For this the intensities measured at 25°C were considered to be correct and the difference between $F_{obs.}$ and $F_{calc.}$ was assumed to be the magnitude of the error affecting each reflection. This correction was applied to the high-temperature data and a subsequent cycle of anisotropic refinement rapidly converged to $R = .054$ ($F > 2$).At this point a difference Fourier synthesis showed no anomalies. The final values of the atomic coordinates and their standard deviations both at 24° and 75° are given in Table 2.

## Results and discussion

### Structure description

Selected interatomic distances are listed in Table 3 for the high- and low-temperature structures. For a detailed description of the structure, the reader is referred to the article by BIRLE *et al.* (1968) on forsterite. Only sufficient information will be given here in order to provide background for the ensueing discussion.

The structure can be visualized as an infinite chain of cations aligned along the *c* axis, which are coordinated both tetrahedrally and octahedrally by fluorine atoms. Two types of octahedral sites are present: M(1) (located on inversion centers) and M(2), having point symmetries, respectively, approximately $D_{4h}$ and $C_v$. Beryllium-centered tetrahedra link the chains of octahedra and determine the *a* translation. Each octahedral chain lies on the voids determined by the previous ones. Due to the small size of the beryllium atom (crystal radius = .89 Å), its high ionization potential (9.32 eV) and its high sublimation energy, the beryllium-to-fluorine bonds are considered to be of a $sp^3$ type. Most likely an optimal interrelationship between ionic and covalent forces, packing requirements and preferential directions of thermal vibration accounts for the asymmetries of the atomic positions as shown by the distortions of the M(1) and M(2) polyhedra. Some positional parameters at 25 ° and 74 °C are equal within their standard deviation. However, a comparison of the bond lengths shows that the changes taking place upon heating are real and of considerable magnitude, both in the tetrahedral and octahedral groups. Figure 2 shows a portion of the serrated chains projected down the *a* axis.

### Thermal vibration

Since $\gamma$ $Na_2BeF_4$ has four molecules per unit cell, acoustic and optical modes of vibration affect the structure. Computation of the root-mean-square amplitudes from the values of the artificial isotropic temperature factors *B*, shows an increase with temperature for all the atoms with the exception of Na(2) and F(1). This relation is better seen by a comparison of the tensors *U*, computed from the fractional parameters of the anisotropic temperature factors according to the equation

$$U = \frac{1}{2\pi^2} \Sigma \frac{\beta_{ij}}{a_{ij}^{2*}},$$

where the $a_{ij}$'s are the cell parameters.

Table 3. *Selected interatomic distances at 25° and 74°C*

| Atom pair | 25°C | 74°C | Δ |
|---|---|---|---|
| | | Beryllium tetrahedron | |
| Be—F(1) | 1.5475 (3) Å | 1.5761 (2) Å | 0.02860 Å |
| —F(2) | 1.5739 (1) | 1.5269 (1) | — 0.0470 |
| 2 —F(3) | 1.5525 (2) | 1.5481 (2) | — 0.0044 |
| mean | 1.557 | 1.550 | |
| F(1)—F(2) | 2.5720 (3) | 2.5668 (3) | 0.0052 |
| 2 —F(3) | 2.5816 (3) | 2.5859 (3) | 0.0043 |
| 2 F(2)—F(3) | 2.5016 (2) | 2.4746 (1) | — 0.0270 |
| mean | 2.551 | 2.542 | |
| | | M(1) octahedron | |
| 2 Na(1)—F(1) | 2.3107 (3) | 2.3057 (2) | — 0.0050 |
| 2 —F(2) | 2.2526 (3) | 2.2432 (2) | — 0.0094 |
| 2 —F(3) | 2.3447 (2) | 2.3518 (2) | 0.0071 |
| mean | 2.302 | 2.300 | |
| 2 F(1)—F(2) | 3.1000 (4) | 3.0687 (4) | — 0.0313 |
| 2 —F(2) | 3.3492 (7) | 3.3585 (5) | 0.0094 |
| 2 —F(3) | 3.4544 (3) | 3.4609 (2) | 0.0065 |
| 2 F(2)—F(3) | 3.1032 (4) | 3.1283 (3) | 0.0251 |
| —F(3) | 2.5016 (2) | 2.4746 (1) | — 0.0270 |
| mean | 3.101 | 3.098 | |
| | | M(2) octahedron | |
| Na(2)—F(1) | 2.3699 (2) | 2.3716 (1) | 0.0017 |
| —F(2) | 2.3426 (1) | 2.2752 (1) | 0.0326 |
| 2 —F(3) | 2.3113 (4) | 2.3161 (3) | 0.0048 |
| 2 Na(2)—F(3) | 2.3806 (2) | 2.3811 (2) | 0.0005 |
| mean | 2.326 | 2.336 | |
| 2 F(1)—F(3) | 3.1210 (4) | 3.1171 (4) | 0.0039 |
| —F(3) | 3.3789 (3) | 3.3859 (2) | 0.0070 |
| 2 F(2)—F(3) | 3.5661 (2) | 3.5926 (2) | 0.0265 |
| 1 F(3)—F(3) | 2.5015 (5) | 2.4914 (4) | — 0.0101 |
| 1 —F(3) | 3.2185 (3) | 3.2190 (3) | 0.0005 |
| 1 F(3)—F(3) | 4.0674 (3) | 4.0855 (3) | 0.0181 |
| mean | 3.279 | 3.288 | |
| | | F(1) bonds | |
| 1 F(1)—Be | 1.5475 (3) | 1.5761 (2) | 0.0286 |
| 2 —Na(1) | 2.3107 (2) | 2.3057 (2) | — 0.0050 |
| —Na(2) | 2.3699 (2) | 2.3716 (1) | 0.0017 |

Table 3. *(Continued)*

| Atom pair | 25 °C | 74 °C | $\Delta$ |
|---|---|---|---|
| | | F(2) bonds | |
| F(2)—Be | 1.5739 (1) | 1.5269 (1) | — 0.0470 |
| 2 —Na(1) | 2.2526 (3) | 2.2432 (2) | — 0.0094 |
| —Na(2) | 2.2426 (1) | 2.2752 (1) | 0.0326 |
| | | F(3) bonds | |
| F(3)—Be | 1.5525 (2) | 1.5481 (2) | — 0.0044 |
| —Na(1) | 2.3447 (2) | 2.3518 (2) | 0.0071 |
| —Na(2) | 2.3113 (4) | 2.3161 (3) | 0.0048 |
| —Na(2) | 2.3806 (2) | 2.3811 (2) | 0.0005 |

A quantitative analysis of thermal vibration could be pursued from a study of the $U$'s by considering the sodium and beryllium atoms acting as rigid bodies on the fluorines. Unfortunately a suitable computer program capable of reliable analyses for three-dimensional close-packed structures is not available. However, on a qualitative level, inspection of Table 4 suggests that thermal vibration is mostly librational. Figures 3 and 4 show a plot of the temperature dependence of the $U$'s for Be and F(3); it can be seen that Be is considerably affected by the temperature change and vibrates preferentially along $U_{11}$. Due to restrictions imposed by symmetry-fixed positions and aside from

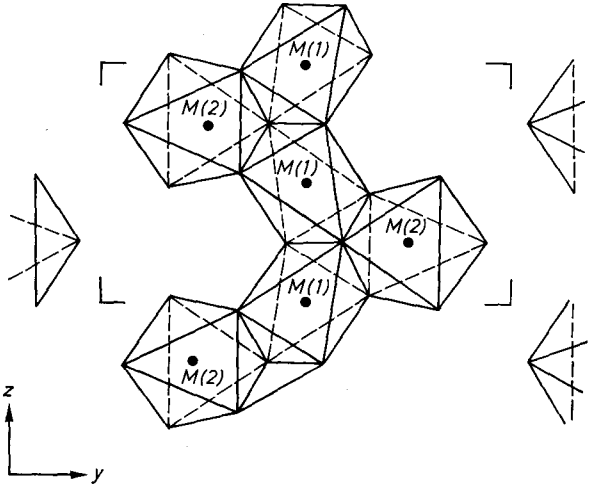


Fig. 2. The crystal structure of $\gamma$ $Na_2BeF_4$ projected down the $a$ axis

Table 4. *Values of the U's at room and high temperature*

| | 25°C | 74°C | $\Delta U$ |
|---|---|---|---|
| Na(1) | | | |
| $U_{11}$ | 0.01578 | 0.01984 | + 0.00406 |
| $U_{22}$ | 0.02903 | 0.0264 | − 0.0026 |
| $U_{33}$ | 0.02012 | 0.0200 | − 0.00012 |
| $U_{12}$ | − 0.0021 | − 0.00027 | − 0.0018 |
| $U_{13}$ | − 0.0021 | − 0.0006 | − 0.0015 |
| $U_{23}$ | − 0.0047 | − 0.0054 | + 0.0007 |
| Na(2) | | | |
| $U_{11}$ | 0.0161 | 0.0145 | − 0.0016 |
| $U_{22}$ | 0.0157 | 0.01210 | − 0.0036 |
| $U_{33}$ | 0.0297 | 0.02958 | − 0.00012 |
| $U_{12}$ | 0.000081 | 0.00130 | + 0.0012 |
| Be | | | |
| $U_{11}$ | 0.00679 | 0.0150 | + 0.00821 |
| $U_{22}$ | 0.0139 | 0.0151 | + 0.0012 |
| $U_{33}$ | 0.0234 | 0.023449 | + 0.000049 |
| $U_{12}$ | 0.00081 | − 0.00406 | − 0.00324 |
| F(1) | | | |
| $U_{11}$ | 0.0094 | 0.0064 | − 0.003 |
| $U_{22}$ | 0.0260 | 0.0242 | − 0.0018 |
| $U_{33}$ | 0.0308 | 0.03068 | − 0.00012 |
| $U_{12}$ | − 0.0000541 | 0.00108 | + 0.00102 |
| F(2) | | | |
| $U_{11}$ | 0.0149 | 0.0199 | + 0.005 |
| $U_{22}$ | 0.01572 | 0.0150 | − 0.0042 |
| $U_{33}$ | 0.0288 | 0.02893 | + 0.00012 |
| $U_{12}$ | − 0.00078 | − 0.00542 | + 0.0046 |
| F(3) | | | |
| $U_{11}$ | 0.0167 | 0.0199 | + 0.0032 |
| $U_{22}$ | 0.0223 | 0.0163 | − 0.006 |
| $U_{33}$ | 0.0212 | 0.0234 | + 0.0022 |
| $U_{12}$ | 0.0014 | 0.00108 | − 0.00032 |
| $U_{13}$ | 0.0005 | 0.0007 | + 0.0002 |
| $U_{23}$ | 0.0036 | 0.0069 | + 0.0033 |

considerations of nearest-neighbor interactions which are particularly effective in a close-packed structure, only F(3) can be chosen as an indicator of the phononic disturbance affecting the structure. However

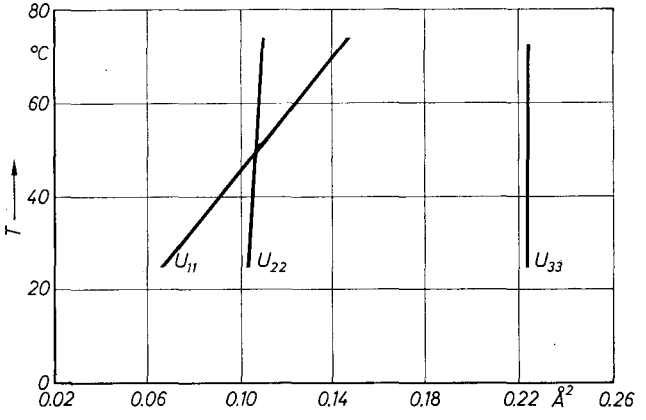


Fig. 3. Temperature dependence of the $U$'s for the Be atom

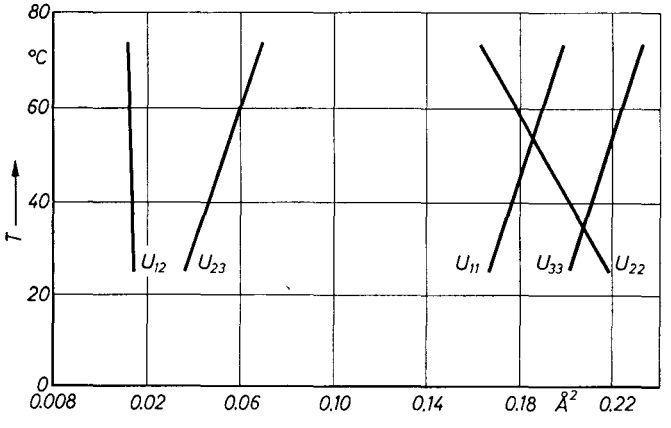


Fig. 4. Temperature dependence of the $U$'s for the F(3) atom

the temperature dependence of the F(3) tensorial components is not in agreement with the experimental values of thermal expansion (Table 1). This is more readily seen by considering the values of the root-mean-square amplitudes referred to both the principal directions of the trivariate normal-distribution function and the crystallographic axes (Table 5). Examination of the data relative to the other atoms fails to substantiate such a direct correlation, thus indicating that variation of the values of the $U$'s should be more realistically considered in connection with changes of orientation of the groups and with changes in interatomic distances. On an absolute scale the principal axis, (3), is a preferential direction of thermal vibration, the magnitude of which

Table 5. *Root-mean-square amplitudes and direction cosines at room and high temperature*

| Atom | 25 °C | | | | | 74 °C | | | | |
|---|---|---|---|---|---|---|---|---|---|---|
| | rms amplitude | rms cryst. axis | Direction cosines | | | rms amplitude | rms cryst. axis | Direction cosines | | |
| Na(1) | 0.1176 Å | 0.1256 | 0.8322 | 0.2696 | 0.4844 | 0.1301 Å | 0.1406 | 0.1923 | 0.4844 | 0.8534 |
| | 0.1411 | 0.1703 | − 0.5489 | 0.2783 | 0.7881 | 0.1410 | 0.1613 | 0.9813 | − 0.0955 | − 0.1669 |
| | 0.1765 | 0.1418 | − 0.077 | 0.9218 | − 0.3796 | 0.1700 | 0.1412 | 0.0006 | 0.8696 | − 0.4937 |
| Na(2) | 0.1253 | 0.1253 | 0.0 | − 1.0 | 0.0 | 0.1081 | 0.1207 | 0.3530 | − 0.9355 | 0.0 |
| | 0.1270 | 0.1253 | − 0.999 | 0.0 | 0.1223 | 0.1224 | 0.1100 | − 0.9356 | − 0.3530 | 0.0 |
| | 0.1724 | 0.1724 | 0.0 | 0.0 | − 0.999 | 0.1720 | 0.1720 | 0.0 | 0.0 | 0.0 |
| Be | 0.0818 | 0.0824 | − 0.9936 | 0.1121 | 0.0 | 0.1072 | 0.1207 | − 0.4045 | − 0.9145 | 0.0 |
| | 0.1183 | 0.1183 | − 0.1121 | − 0.9936 | 0.0 | 0.1231 | 0.1100 | − 0.9145 | 0.4045 | 0.0 |
| | 0.1529 | 0.1529 | 0.0 | 0.0 | − 0.999 | 0.1531 | 0.1531 | 0.0 | 0.0 | − 1.0 |
| F(1) | 0.0972 | 0.0972 | 0.999 | 0.0 | 0.0 | 0.0779 | 0.0779 | 1.0 | 0.0 | 0.0 |
| | 0.1612 | 0.1612 | 0.0 | 1.0 | 0.0 | 0.1631 | 0.1631 | 0.0 | 1.0 | 0.0 |
| | 0.1755 | 0.1755 | 0.0 | 0.0 | 0.999 | 0.1751 | 0.1751 | 0.0 | 0.0 | 1.0 |
| F(2) | 0.1210 | 0.1221 | 0.8918 | 0.4522 | 0.0 | 0.0935 | 0.1393 | − 0.4527 | − 0.8916 | 0.0 |
| | 0.1264 | 0.1253 | − 0.4522 | 0.8918 | 0.0 | 0.1489 | 0.1072 | 0.8916 | − 0.4527 | 0.0 |
| | 0.1698 | 0.1698 | 0.0 | 0.0 | 0.999 | 0.1700 | 0.1700 | 0.0 | 0.0 | − 1.0 |
| F(3) | 0.1263 | 0.1294 | − 0.8617 | 0.3755 | − 0.3409 | 0.1091 | 0.1393 | 0.1658 | − 0.8416 | 0.5139 |
| | 0.1372 | 0.1495 | − 0.5004 | − 0.5194 | 0.6926 | 0.1401 | 0.1278 | − 0.9861 | − 0.1410 | 0.0873 |
| | 0.1597 | 0.1456 | − 0.0830 | − 0.7675 | − 0.6356 | 0.1663 | 0.1531 | − 0.0010 | − 0.5212 | − 0.8533 |

progressively decreases along the other principal directions, (2) and (1), of the atomic thermal ellipsoids. Such a relationship does not hold for the two latter axes if referred, respectively, to the crystallographic translations $b$ and $a$, thus stressing the expected anisotropic behavior of the frequency of the thermal waves.

## The beryllium tetrahedron

Figure 5 shows that the temperature change considerably affects the beryllium tetrahedron. The Be—F(2) bond length, parallel to $b$, shortens from 1.574 to 1.527 Å, whereas Be—F(1), parallel to $a$, increases from 1.547 to 1.576 Å. Although the interatomic distances

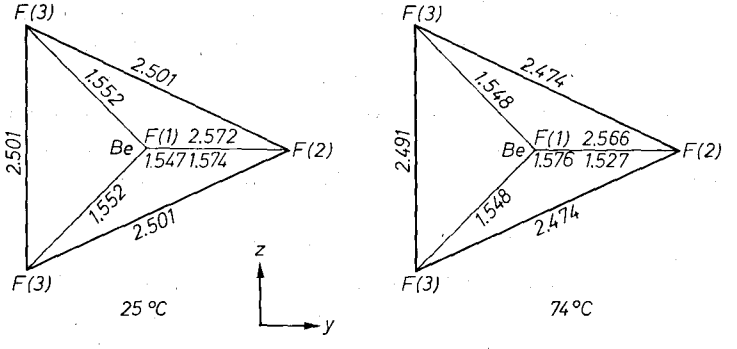


Fig. 5. The beryllium tetrahedron at 25° and 74 °C

between the beryllium atom and the coordinated fluorines decrease, the relative bond lengths between the anions are little affected along $b$ and $c$. The F(3)—F(3) and F(1)—F(2) bonds, respectively parallel to $c$ and $b$ decrease from 2.501 to 2.491 Å. In agreement with the Be—F(1) contraction, the bond F(3)—F(2) decreases from 2.501 to 2.474 Å. The net effect of these changes is a slight contraction along $c$ and $b$ and expansion along $a$.

## The M(1) octahedron

The M(1) octahedron has the coordinating cation fixed at an inversion center and is spatially controlled by two $(BeF_4)^=$ groups. Since F(1) is located in the center of gravity of the groups [the angle F(1)—Na(2)—F(1) is 180 °] and adjacent layers are linked by vertex sharing of octahedra, it might be reasonable to suggest, on a qualitative basis, that any induced stress in the system should tend to lock

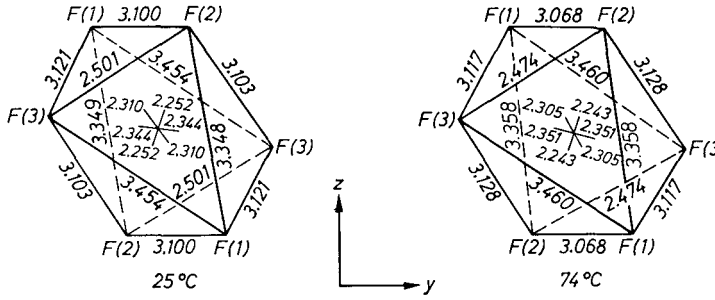


Fig. 6. The M(1) octahedron at 25° and 74 °C

it in position, thus explaining the decrease of the artificial temperature parameter $B$ at 74 °C. The previously mentioned contraction of the F(3)—F(2) tetrahedral bonds reduces the F(1)—F(2) distance from 3.100 to 3.068 Å. Although no major contribution to thermal expansion is expected from this group due to its symmetry-fixed configuration, a minor reorientation takes place since the octahedron pivots on F(1) and slightly expands along $b$ and $c$. The results are shown in Fig. 6.

## The M(2) octahedron

Due to the tetrahedral contraction along F(1)—F(3) and the resultant shortening of the F(3)—F(3) bond from 2.501 to 2.491 Å, the M(2) octahedron expands along the bond F(3)—F(3) from 4.067 to 4.085 Å. This expansion is parallel to $c$ and is only a fraction of the total thermal displacement in this direction. The bond Na(2)—F(2) which is parallel to $b$ significantly increases from 2.242 to 2.275 Å and since this increase is directly related to the contraction of the Be—F(2) bond of the tetrahedral groups, it provides an excellent example of cationic repulsion. The results are diagrammatically shown in Fig. 7.

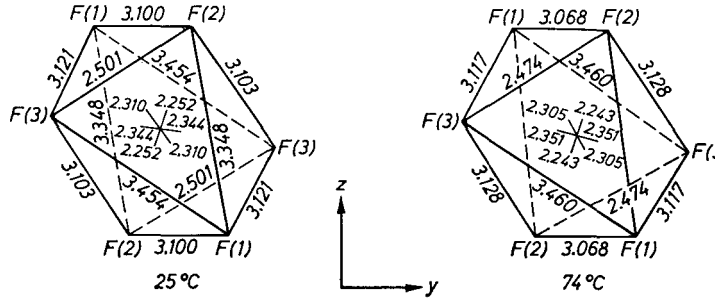


Fig. 7. The M(2) octahedron at 25° and 74 °C

## Mechanism of thermal expansion

Thermal expansion depends upon the potential energy function, the behavior of which can be, at most, satisfactorily approximated in case of a pair potential between atoms. In real crystals such a model is inadequate. Theoretical approaches leading to a computation of the energy function are further complicated by the strong anisotropy associated with non-central forces such as directional valence bonds or by effects of phonon-electron interaction. Even the experimental values of the root-mean-square amplitudes as deduced by routine structural methods are inadequate for quantitative analysis, since the frequency of thermal vibration is, at most, of the order of $10^{-13}$ sec as compared to $10^{-18}$ sec for x-rays. Although such restrictions do not appear to allow a quantitative prediction of the thermal expansion behavior, there is evidence in the data for $\gamma$ $Na_2BeF_4$ which allows at least a qualitative explanation to be formulated. According to the values of the root-mean-square amplitudes at 25° and 74 °C, $c$ is the preferential direction of stress relief. Expansion along this direction can be visualized as a cumulative vibrational effect which affects a direction of high electron density, characterized by complex phenomena of electron-phonon interaction.

Expansion along $b$ is controlled by the M(1) cations located on inversion centers and, because of this point symmetry, translational motions along this direction are restricted. The main contribution to expansion along $b$ appears to be associated with the increase of the Na(2)—F(1) distance in the M(2) sites due to cationic repulsions from the anharmonic pair potential due to Na and Be.

On theoretical grounds, expansion along $a$ should be the smallest since it should be controlled by the stability of the tetrahedral configuration which links the chains along this direction. This is in agreement with the experimental results (Table 1 and Fig. 1). However, at 74 °C a major change appears to affect the tetrahedral bonds. Decrease of the Be—F(2) bond length enhances the $s$ character of the beryllium orbital along $b$ and correspondingly increases the $p$ character of the antisymmetrical bond Be—F(1) which thus becomes more covalent. According to PAULING's theory on the partial ionic character of covalent bonds, the change can be semiquantitatively computed according to the equation

$$\text{Ionic character} = 1 - e^{-1/4\,(X_A - X_B)},$$

where $X_A$ and $X_B$ are the electronegativities of the elements under con-

sideration. This gives a value of 0.75 for a pure $p$ and of 0.28 for a pure $s$ character of the beryllium orbital. The difference of these two values can be interpreted as causing a preferential direction of polarization along $a$ due to the formation of a stronger repulsion potential along this direction. This process appears to be directly related to the abrupt increase in $\alpha_1$ at 120 °C. According to the available data, if uniformity of expansion (and contraction) of the bonds is assumed upon heating, at 120 °C the tetrahedral distance Be—F(1) should be considerably weakened due to a change from a $sp^3$ configuration to one tending toward lower values of orbital hybridization. This would imply smaller tetrahedral angles, less stability of the structure and an increase in polarization along $a$. The magnitude of the polarization would thus be sufficiently high to partly overcome the spatial limitations imposed by the packing of the serrated chains. This process opposes the close-packed arrangement and at a critical temperature a phase change should take place. This is in agreement with the experimental data since at $187 \pm 5$ °C an inversion to a monoclinic phase was found. Existence of such a phase change is in agreement with a trend that appears to require orthorhombic close-packed structures to invert to monoclinic symmetry as a result of a drastic increase of the potential energy of the structure (AMORÓS *et al.*, 1968).

## Acknowledgements

I wish to express my sincere thanks to Prof. J. V. SMITH for his criticism while this work was carried out under his guidance. Special thanks are due to Prof. P. B. MOORE and Dr. I. STEELE respectively, for advice and help in collecting the data and improving the manuscript. Prof. HINZE gave a valuable insight into the mechanism of expansion of the bonds. The National Science Foundation grants GA-572 and GA-2123 for research support and a fellowship from the Owens Illinois Glass Company are gratefully acknowledged.

### References

J. L. AMORÓS and M. AMORÓS (1968), *Molecular crystals*. J. Wiley & Sons.

J. D. BIRLE, G. V. GIBBS, P. B. MOORE and J. V. SMITH (1968), Crystal structures of natural olivines. Amer. Mineralogist **53**, 807—824.

W. R. BUSING, K. O. MARTIN and H. A. LEVY (1962), ORFLS, a FORTRAN crystallographic least squares program. U. S. Atomic Energy Commission Report No. ORNL-TM-305.

W. J. CAMPBELL (1962), Platinum expansion values for thermal calibration of high temperature x-ray diffraction cameras and diffractometers. U.S. Bureau of Mines, Information Circular number 8107.

H. CHESSIN, W. C. HAMILTON and B. POST (1965), Position and thermal parameters of oxygen atoms in calcite. Acta Crystallogr. **18**, 689–693.

K. HANKE (1965), Beiträge zu Kristallstrukturen vom Olivin-Typ. Beitr. Mineral. Petrogr. **11**, 535–558.

C. H. MACGILLAVRY and G. D. RIECK (1962), *International tables for x-ray crystallography*, Vol. 3. The Kynoch Press, Birmingham.

L. PAULING (1960), *The nature of the chemical bond.* Cornell University Press, p. 98.

W. H. ZACHARIASEN (1965), Multiple diffraction in imperfect crystals. Acta Crystallogr. **18**, 705.